

PACS numbers: 32.80.Fb; 32.80.Dz
DOI: 10.1070/QE2005v035n01ABEH002787

Photoionisation of a helium atom involving autoionisation states coupled by a circularly polarised laser field

E.V. Gryzlova, A.I. Magunov, I. Rotter, S.I. Strakhova

***Abstract*. The rotating wave approximation is used to obtain parametric expressions for the resonance cross section for the atomic ground state ionisation by linearly polarised probe radiation in the vicinity of an autoionisation state coupled resonantly to another autoionisation state through circularly polarised laser radiation. Calculations are made for the $2s2p\,^1P$ and $2s3d\,^1D$ states of the helium atom. It is shown that the structure of the photoionisation cross-section spectrum formed for circularly polarised laser radiation differs qualitatively from the structure formed in the case of linear polarisation. The dependence of this structure on the intensity and frequency of laser radiation and the direction of polarisation of the probe radiation is studied.**

Keywords: *polarisation phenomena, interference effects, helium spectrum, autoionisation states.*

1. Introduction

Resonance interaction of laser radiation with atoms induces a variety of interference phenomena. Investigations of resonance effects in the vicinity of autoionisation states (AISs) are of special interest. Apart from the known interference of direct and resonance transitions to the continuous spectrum leading to the asymmetry of the absorption line, which was described by Fano [1], an additional mixing of levels by laser radiation leads to a considerable modification of the resonance structure. The shape of the resonance structure depends on the laser radiation intensity and frequency. Experimental investigations of AISs of various atoms were performed mainly using linearly polarised laser radiation [2, 3]. Theoretical analysis and calculations under the same conditions were made for AISs coupled resonantly with a laser field [4 – 9] and laser-induced resonances in a continuum [10 – 13].

The important role of polarisation was highlighted even in the pioneering work [14], where circularly and linearly polarised laser fields were used to detect laser-induced resonances in the continuum spectrum of cesium atoms. Later, this technique was also used for other atoms [15, 16]. It is reasonable to assume that laser radiation polarisation can also exert a considerable effect on the interference structure formed in the case of resonance coupling of AISs.

In this paper, we study the ionisation from the $1s^2\,^1S$ ground state of a helium atom by a probe VUV radiation with a wavelength corresponding to a single-photon transition to the $2s2p\,^1P$ AIS coupled with the $2s3d\,^1D$ AIS through circularly polarised laser radiation that is often called pump radiation. The detuning $\delta = \omega - (E_D - E_P)/\hbar$ of the pump frequency ω from the resonance is comparable with the autoionisation rate. The interference structure of the photoionisation cross section was studied earlier while considering the dependence of identical linear polarisations of the pump and probe radiation [6, 8] on the pump intensity and frequency. The aim of this paper is to study the effect of pump radiation polarisation on the interference structure.

Figure 1 shows the diagram of resonantly coupled magnetic sublevels of the AIS of the helium atom. The selection rules for transitions between the magnetic sublevels M are determined by the polarisation of the pump field. If the quantisation axis is chosen in the direction of the wave vector $\boldsymbol{k}$, the $2s2p\,^1PM \leftrightarrow 2s3d\,^1D(M+1)$ transitions for the right-hand polarisation and the $2s2p\,^1PM \leftrightarrow 2s3d\,^1D(M-1)$ transitions for the left-hand polarisation of the field are possible. In addition, one-photon ionisation of the upper AIS by laser radiation to the continuum above the second threshold of single ionisation ($2s3d \rightarrow 2lEl'$) is also possible. One-photon ionisation of both AISs to the $1sEl$ channels by the pump radiation can be neglected because of a small overlap of one-electron orbitals 1s and 2s. The rates of AIS ionisation by the probe field are negligible due to its low intensity. We consider two cases corresponding to the direction of linear polarisation of the probe radiation along the pump wave vector and perpendicular to it.

Unless stated otherwise, atomic units are used throughout this work.

2. Theory

In the dipole approximation, the wave function of an atom in an electromagnetic field is determined by solving the nonstationary Schrödinger equation

E.V. Gryzlova Department of Physics, M.V. Lomonosov Moscow State University, Vorob'evy gory, 119992 Moscow, Russia; e-mail: Gryzlova@mail333.com;
A.I. Magunov A.M. Prokhorov General Physics Institute, Russian Academy of Sciences, ul. Vavilova 38, 119991 Moscow, Russia; e-mail: magunov@fpl.gpi.ru;
I. Rotter Max-Planck-Institut für Physik Komplexer Systeme, D-01187 Dresden, Germany;
S.I. Strakhova D.V. Skobel'tsyn Institute of Nuclear Physics, M.V. Lomonosov Moscow State University, Vorob'evy gory, 119992 Moscow, Russia; e-mail: str@sinp.msu.ru

Received 6 July 2004; revision received 9 November 2004
Kvantovaya Elektronika **35** (1) 43 – 47 (2005)
Translated by Ram Wadhwa

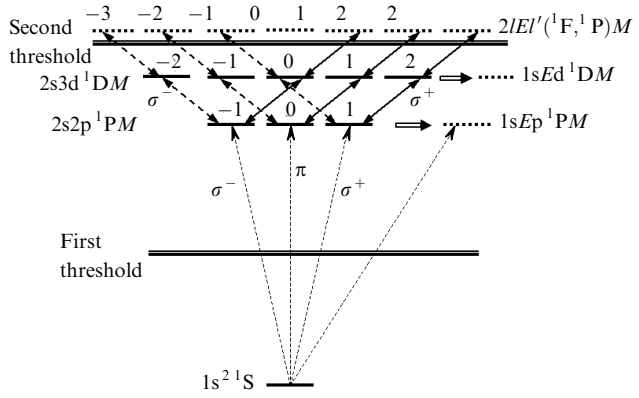

Figure 1. Scheme of resonance transitions between the magnetic sublevels 2s2p ^{1}P and 2s3d ^{1}D of the AIS, induced in the helium atom by circularly polarised laser radiation. The axis of quantisation of the projection of angular momentum M is directed along the wave vector $\boldsymbol{k}$. Thin arrows indicate transitions from the ground state caused by probe field with linear (π) and circular ($\sigma^{\pm}$) polarisations (superposition of σ^+ and σ^- results in linear polarisation perpendicular to $\boldsymbol{k}$); double arrows indicate autoionisation transitions; and two-way (dashed and solid) arrows show one-quantum transitions σ^+ and σ^-. One-photon transitions to the continuum above the second threshold of single ionisation from the 2s3d ^{1}DM AIS make additional contribution to their total width; coupled–free dipole transitions between first and second thresholds are weak and not shown in the scheme; E is the energy of the state.

$$\mathrm{i}\frac{\partial \Psi}{\partial t} = \left[\hat{H}_0 - \boldsymbol{D}\cdot\boldsymbol{F}(t) - \boldsymbol{D}\cdot\boldsymbol{f}(t)\right]\Psi(t),$$
$$\Psi(t\to-\infty)\to\exp(-\mathrm{i}E_\mathrm{g}t)\Phi_\mathrm{g}, \tag{1}$$

where $\hat{H}_0$ is the Hamiltonian of a free atom, $\boldsymbol{D}$ is the dipole moment operator, and Φ_g is the wave function of the ground state of the atom. The strength of the circularly polarised electric pump field is

$$\boldsymbol{F}_\lambda(t) = \frac{F(t)}{\sqrt{2}}\left[\boldsymbol{n}_x\cos(\omega t) + \lambda\boldsymbol{n}_y\sin(\omega t)\right]$$
$$= \frac{F(t)}{2}\left[\boldsymbol{n}_{-1}\exp(\mathrm{i}\lambda\omega t) - \boldsymbol{n}_1\exp(-\mathrm{i}\lambda\omega t)\right], \tag{2}$$

where $\lambda = 1$ and -1 correspond to the right- and left-hand polarisations, respectively; and $\boldsymbol{n}_{\pm1} = \mp(\boldsymbol{n}_x \pm \mathrm{i}\boldsymbol{n}_y)/2^{1/2}$ and $\boldsymbol{n}_0 = \boldsymbol{n}_z$ are the cyclic unit vectors. The probe radiation is linearly polarised in the direction of the unit vector $\boldsymbol{\varepsilon}$:

$$\boldsymbol{f}(t) = f(t)\boldsymbol{\varepsilon}\cos(\Omega t). \tag{3}$$

We assume that the laser pulse duration is considerably longer than the lifetime of AISs and the probe pulse duration. In this case, ionisation from the ground state caused by a weak probe radiation which can be described by the first-order perturbation theory, occurs at a fixed laser field strength. We neglect multiphoton ionisation and free–free transitions induced by a laser field assuming that the field intensity is not high enough for them.

Following [8, 9], we can obtain in the rotational wave approximation the expression for the non-Hermitian effective Hamiltonian describing the evolution of the pairwise coupled magnetic sublevels 2s2p ^{1}P and 2s3d ^{1}D AIS in the helium atom:

$$\boldsymbol{H}_\mathrm{eff} = \begin{bmatrix} \boldsymbol{H}_{-1} & [0] & [0] \\ [0] & \boldsymbol{H}_0 & [0] \\ [0] & [0] & \boldsymbol{H}_1 \end{bmatrix}, \tag{4}$$

where

$$\boldsymbol{H}_M = \begin{bmatrix} E_\mathrm{P} - \frac{\mathrm{i}}{2}\Gamma_\mathrm{P} & (d_{\lambda M})^* I_\mathrm{las}^{1/2} \\ d_{\lambda M} I_\mathrm{las}^{1/2} & E_\mathrm{D} - \omega - \frac{\mathrm{i}}{2}(\Gamma_\mathrm{D} + \gamma_{\lambda M} I_\mathrm{las}) \end{bmatrix}; \tag{5}$$

$M = -1, 0, 1;$

E_L and Γ_L is the energy and width of the AIS, respectively; $d_{\lambda M} = \langle \mathrm{D}M + \lambda | D_\lambda | \mathrm{P}M\rangle$ is the matrix element of the cyclic component of the dipole moment; $\gamma_{\lambda M} I_\mathrm{las} = 2\pi\sum_{El}|\langle El(M+2\lambda)|D_\lambda|\mathrm{D}M+\lambda\rangle|^2 I_\mathrm{las}$ is the laser-induced width of the ^{1}D AIS; and $I_\mathrm{las} = F^2/4$ is the pump intensity.

The complex eigenvalues of the non-Hermitian effective Hamiltonian (4) have the form

$$\tilde{E}_M^{(\pm)} = \frac{1}{2}\Bigg[E_\mathrm{P} + E_\mathrm{D} - \omega - \frac{\mathrm{i}}{2}(\Gamma_\mathrm{P} + \Gamma_\mathrm{D} + \gamma_{\lambda M} I_\mathrm{las})$$
$$\pm \frac{1}{2}\left\{\left[\delta - \frac{\mathrm{i}}{2}(\Gamma_\mathrm{P} - \Gamma_\mathrm{D} - \gamma_{\lambda M} I_\mathrm{las})\right]^2 + 4|d_{\lambda M}|^2 I_\mathrm{las}\right\}^{1/2}. \tag{6}$$

Unlike the diagonal matrix elements $\boldsymbol{H}_\mathrm{eff}$, the eigenvalues of Hamiltonian (6) determine the experimentally observed positions and widths of resonances. Nondiagonal elements in (5), which couple the AISs are Hermite conjugate. For the discrete states ($\Gamma_\mathrm{P,D} = 0$; $\gamma_{\lambda M} = 0$), they cause a splitting of the energies of bound states by an amount equal to the Rabi frequency $2|d_{\lambda M}|I_\mathrm{las}^{1/2}$ [17].

The energy level diagram presented in Fig. 1 and the symmetry properties of the transition matrix elements show that the left- and right-hand polarisations of pump radiation lead to the same result for the cross sections of ionisation by linearly polarised probe radiation. The following analysis will be carried out for the right-hand polarised pumping.

In the presence of resonance laser radiation, the photoionisation cross section has the form

$$\sigma(\Omega,\omega,I_\mathrm{las}) = \sum_{M=-1}^{1}\sigma_M^{(\mathrm{d})}(\Omega)\left\{1 - \mathrm{Im}\left[\boldsymbol{t}_M^\mathrm{T}(\Omega\boldsymbol{I} - \boldsymbol{H}_M)^{-1}\boldsymbol{t}_M\right]\right\}, \tag{7}$$

where $\sigma_M^{(\mathrm{d})}(\Omega)$ is the partial cross section for direct ionisation by probe radiation at frequency Ω for projection of the magnetic moment M; $\sigma_\mathrm{d} = \sum_M \sigma_M^{(\mathrm{d})}$ is the total cross section; $\boldsymbol{I}$ is a unit 2×2 matrix; and superscript T denotes transposition of the matrix. The two-component vector $\boldsymbol{t}_M$ describing transitions from the ground state has a simple form:

$$\boldsymbol{t}_M = \left(\frac{\Gamma_\mathrm{P}}{2}\right)^{1/2}\begin{bmatrix} q - \mathrm{i} \\ 0 \end{bmatrix}, \tag{8}$$

where q is the Fano parameter for the ^{1}P AIS [13]. Note that expression (7) contains contribution from three different groups of photoelectrons. These include electrons with energy $\Omega - E_\mathrm{i1}$ (E_i1 is the first ionisation threshold) formed in the absence of pumping, photoelectrons with energy $\Omega + \omega - E_\mathrm{i1}$ corresponding to two-photon resonance ionisation by probe and laser radiation, as well as the third group of electrons with energy $\Omega + 2\omega - E_\mathrm{i2}$ (E_i2 is the

second ionisation threshold) produced upon three-photon ionisation involving excitation of the residual ion into a state with the principal quantum number $n = 2$.

Taking into account (5) and (8), we can present (7) in a simplified form:

$$\sigma(\Omega, \omega, I_{\rm las}) = \sigma_{\rm d}(\Omega) \times \left[1 - \sum_{M=-1}^{1} {\rm Im}\left(\frac{A_M^{(+)}}{\Omega - \tilde{E}_M^{(+)}} + \frac{A_M^{(-)}}{\Omega - \tilde{E}_M^{(-)}}\right)\right]. \quad (9)$$

Here, the complex amplitudes of the resonances have the form:

$$A_M^{(+)} = \frac{\Gamma_{\rm P}}{2}\,\rho_M^2 (q - {\rm i})^2\,\frac{E_{\rm D} - \omega - {\rm i}(\Gamma_{\rm D} + \gamma_M I_{\rm las})/2 - \tilde{E}_M^{(+)}}{\tilde{E}_M^{(-)} - \tilde{E}_M^{(+)}},$$

$$A_M^{(-)} = \frac{\Gamma_{\rm P}}{2}\,\rho_M^2 (q - {\rm i})^2\,\frac{\tilde{E}_{\rm M}^{(-)} - E_{\rm D} + \omega + {\rm i}(\Gamma_{\rm D} + \gamma_M I_{\rm las})/2}{\tilde{E}_M^{(-)} - \tilde{E}_M^{(+)}}, \quad (10)$$

where $\rho_M^2 = \sigma_M^{(\rm d)}/\sigma_{\rm d}$.

It can be easily verified that with decreasing pump intensity, $\tilde{E}_M^{(+)} \to E_{\rm P} - {\rm i}\Gamma_{\rm D}/2$, $\tilde{E}_M^{(-)} \to E_{\rm D} - \omega - {\rm i}\Gamma_{\rm D}/2$, so that $A_M^{(+)} \to (\Gamma_{\rm P}/2)\rho_M^2(q - {\rm i})^2$ and $A_M^{(-)} \to 0$. As a result, expression (9) assumes the form of the usual Fano formula for an isolated resonance.

If the probe field is polarised along the pump wave vector (i.e., $\varepsilon \,||\, \boldsymbol{k}$), only one term with $M = 0$ remains in (9), as in the case of linear polarisation considered in [8]. In the case of linear polarisation of the probe field, the direction of its wave vector is not so important if the effect of the magnetic component is neglected. Therefore, it can be assumed that for $\varepsilon \perp \boldsymbol{k}$, the probe field also propagates along $\boldsymbol{k}$. In this case, the probe field can be represented as a superposition of right- and left-hand polarised waves, and terms corresponding to transitions from the ^{1}S ground state to the ^{1}P state with moment projections $M = \pm 1$ have the same weight in expression (9). It is important that each term is determined by different values of $d_{\lambda M}$ and $\gamma_{\lambda M}$, and hence the shifts between resonances increase with intensity $I_{\rm las}$.

3. Results of calculations and discussion

Figure 2 shows the dependences of the positions and widths of resonance states on the pump intensity for different values of resonance detuning. In the case of an exact resonance (Fig. 2a) for an intensity lower than a certain critical value, which is characteristic of each resonance pair, these positions coincide and the widths approach each other with increasing intensity. This situation is qualitatively different from that observed during the participation of discrete states ($\Gamma_{\rm P,D} = 0$), when the energies of resonances having the same width are split starting from the zero intensity (Autler–Townes effect) [17, 18]. In this case, the critical point is located at the origin of the axis ($I_{\rm las} = 0$). The critical pump field intensity for the AIS is determined by equating the radicand in (6) to zero. The smallest value of the solution of the quadratic equation corresponds to the critical intensity $I_{{\rm cr},M} \approx (\Gamma_{\rm P} - \Gamma_{\rm D})^2/(16 d_M^2)$ for which the ionisation width is much smaller than the autoionisation widths. For the second solution, the ionisation width exceeds the autoionisation width, and its value $I_{{\rm cr},M} \approx 16 d_M^2/\gamma_M^2$ is ~ 1 a.u., which is beyond the range of applicability of the approach used here, and is therefore of no practical significance. The difference in the intensity values for different pairs of resonances shown in Fig. 2 is

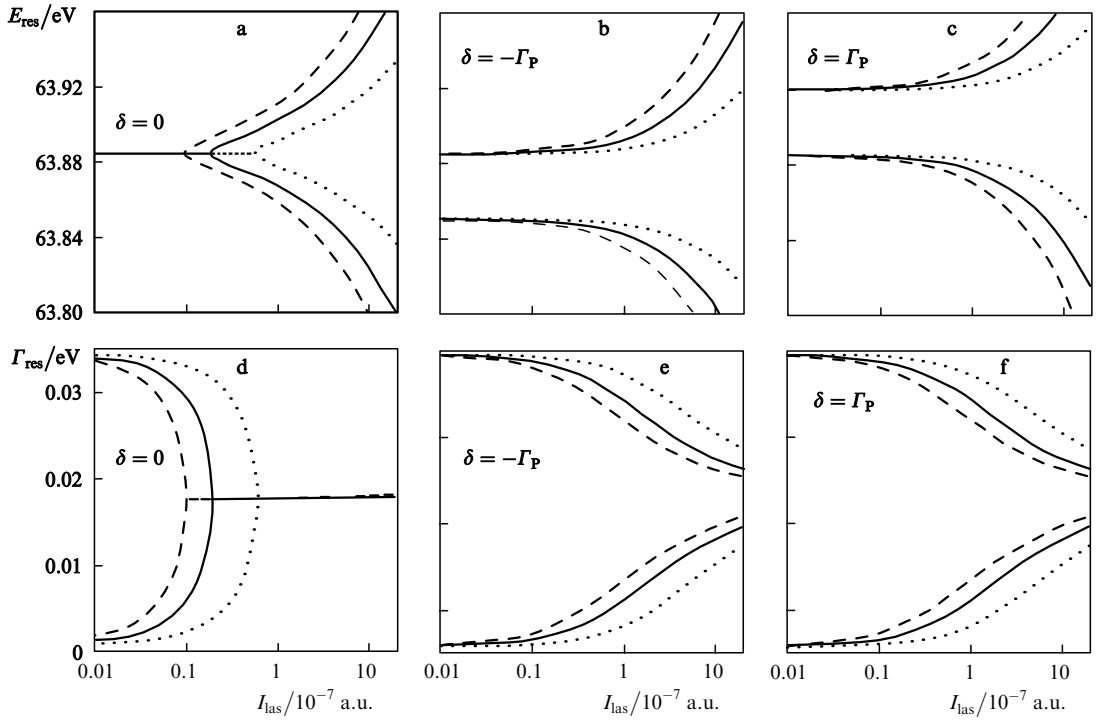

Figure 2. Dependences of the energies and widths of resonances on the intensity of right-hand polarised laser radiation coupling the sublevels $2s2p\,^1{\rm P}M$ and $2s3d\,^1{\rm D}M'$ of the AIS for different detunings δ from the resonance. Solid curves indicate resonances corresponding to $M = 0$, the dashed ones to $M = -1$, and the dotted ones to $M = 1$.

determined by the dependence of the matrix elements of the dipole moment on M (according to the Wigner–Eckart theorem) because they must correspond to the same Rabi frequency.

Figres 3 and 4 show the results of calculations illustrating the effect of pump polarisation on the interference structure of the ionisation cross section in the vicinity of the $2s2p\,^1P$ AIS for different values of the laser field intensity and frequency. The energies and widths of the AIS ($E_P = 2.2159$ a.u., $\Gamma_P = 0.00127$ a.u., $E_D = 2.3477$ a.u., $\Gamma_D = 2.62 \times 10^{-5}$ a.u.), the Fano parameter $q = -2.8$, and the dipole matrix elements are borrowed from [1].

Figure 3 shows the resonance photoionisation cross section for probe radiation polarised linearly in the direction of the pump wave vector as a function of its intensity and resonance detuning. At low intensities, the conventional Fano profile is observed for an isolated resonance. As the intensity increases, the coupling between the sublevels of the states $2s2p\,^1P$ ($M = 0$) and $2s3d\,^1D$ ($M = 1$) also increases, resulting in the appearance of a narrow interference minimum in the ionisation cross section in the case of an exact resonance. Upon a further increase in intensity, the interference structure acquires the shape of two isolated resonances of the same shape with a width about half the autoionisation width of the $2s2p\,^1P$ state. A similar asymptotic behaviour of the cross sections is also observed for a finite detuning of the angular pump frequency from the resonance. For lower intensities, the position and shape of narrow resonances vary strongly according to the sign of detuning. This is due to asymmetry of the Fano profile of the $2s2p\,^1P$ AIS. For $\delta < 0$, a resonance appears in the region of the interference minimum of a broad line, hence its shape is nearly symmetric owing to the absence of interference with the direct ionisation channel and with the transition through the 2s2p state. For $\delta > 0$, the narrow resonance appears at the wing of the broad resonance, and interference with other channels results in a sharp asymmetry in the resonance shape. The cross section behaves in the same way as in the case of linearly polarised pump [8].

A change in the direction of polarisation of the probe radiation results in a qualitative variation of the resonance structure of the absorption cross section. Figure 4 shows the results for linear polarisation of the probe field in a plane perpendicular to the direction of propagation of the pump radiation. In this case, the spectrum exhibits two pairs of resonances corresponding to transitions from the ^1S ground state to the ^1P state with projections $M = 1$ and $M = -1$; the shifts in energy and width depend on the value of M. For high-intensity laser radiation (2×10^{-6} a.u.), all the four resonances are clearly isolated and are similar in shape, as in Fig. 3. The only difference is the height of the resonances, which is reduced to half, so that the energy integrated cross section in both cases is the same as in the absence of the coupling laser field. All these peculiarities follow from the expressions presented above.

Note that in the case of linearly polarised pump, the absorption spectrum of linearly polarised probe radiation contains only two resonances in both the cases considered above. For a mutually perpendicular orientation of pump

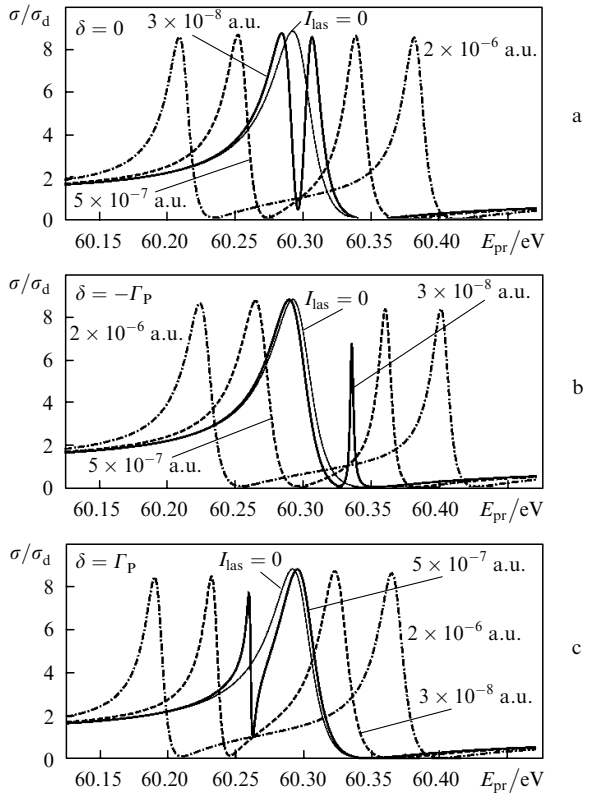

Figure 3. Dependence of the cross sections of resonance photoionisation of a He atom in the vicinity of the $2s2p\,^1P$ AIS on the photon energy E_{pr} of probe radiation for different values of the laser radiation intensity I_{las}, and detuning from the resonance $\delta = \omega + E_P - E_D$. The probe VUV radiation is linearly polarised in the direction of the wave vector $\boldsymbol{k}$.

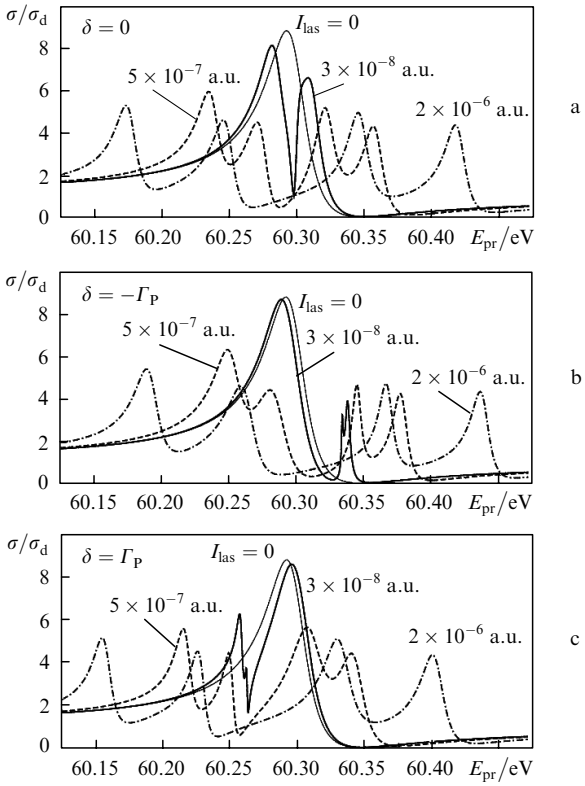

Figure 4. Same as in Fig. 3, but for the probe VUV radiation linearly polarised perpendicular to the wave vector $\boldsymbol{k}$.

and probe field polarisations, the contribution to the cross section comes from two projections $M = \pm 1$ (with the quantisation axis directed along the pump polarisation vector). However, both pairs of resonances corresponding to them are identical because dipole matrix elements and ionisation widths are independent of the sign of the moment projections. For an arbitrary angle between the polarisation vectors, the cross section acquires two more resonances with $M = 0$, corresponding to the transition induced by the probe field component along the pump polarisation. Under such conditions, in the case of circular polarisation (arbitrary angle between ε and $\boldsymbol{k}$), all the six resonances shown in Fig. 2 can be observed in cross section (9).

Figure 5 shows the variation of the resonance structure of the cross section for photoionisation by probe radiation upon a variation of the direction of its linear polarisation as a function of the pump radiation wavelength. The results presented here correspond to various values of detuning of the probe radiation frequency from resonance $\Delta = \Omega + E_S - E_P$ at the $^1S \to {}^1P$ transition. The intensity of laser radiation was set to be 5×10^{-7} a.u. For $\varepsilon \| \boldsymbol{k}$, the line shape is described by the Fano formula, as in the case of linearly polarised laser radiation [8]. For $\varepsilon \perp \boldsymbol{k}$, a more complex structure consisting of two resonances is observed.

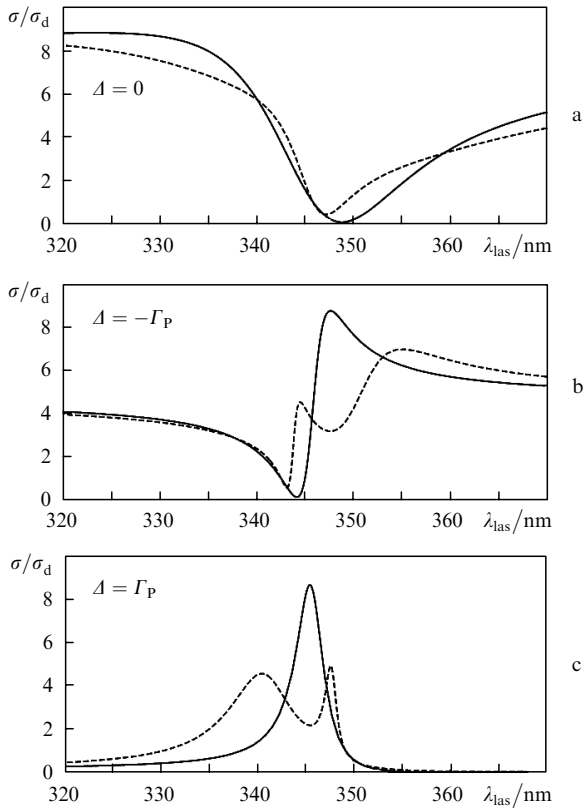

Figure 5. Dependences of the cross section for photoionisation from the ground state of the helium atom in the vicinity of the $2s2p\,^1P$ AIS on the wavelength of circularly polarised laser radiation of intensity $I_{las} = 5 \times 10^{-7}$ a.u., coupling the $2s2p\,^1P$ and $2s3d\,^1D$ AISs for different detunings of the probe radiation frequency from the resonance $\Delta = \Omega + E_S - E_P$. The solid curves correspond to the probe VUV radiation linearly polarised in the direction of the wave vector $\boldsymbol{k}$ of laser radiation, while the dashed curves correspond to the probe field polarised perpendicular to the wave vector $\boldsymbol{k}$.

4. Conclusions

We analysed the effect of polarisation on the resonance structure of the cross section for ionisation by probe radiation in the vicinity of the autoionisation state coupled with another AIS by laser radiation. Analytic expressions are obtained in the rotating wave approximation for ionisation cross section in the case of linearly polarised probe radiation and circularly polarised laser radiation. The position and widths of resonances in the cross section are determined by complex eigenvalues of the effective non-Hermitian Hamiltonian.

The cross sections of resonance photoionisation of a He atom in the vicinity of the $2s2p\,^1P$ state coupled with the $2s3d\,^1D$ AIS are calculated for different values of the laser radiation intensity and detuning of its frequency from the resonance. It is shown that for circularly polarised pump, the ionisation cross section acquires an additional structure that is not present in the case of linearly polarised laser radiation. Depending on the direction of linear polarisation of the probe field, the photoionisation spectrum contains a different number of resonance peaks. A similar peculiarity is also observed in the dependence of the photoionisation cross section on the laser field frequency.

The obtained results can be verified experimentally with the help of currently available synchrotron sources of VUV radiation and lasers providing the required radiation monochromaticity and power.

Acknowledgements. This work was supported by the Russian Foundation for Basic Research (Grant No. 04-02-17236).

References

1. Fano U. *Phys. Rev.*, **124**, 1866 (1961).
2. Karapanagioti N.E., Charalambidis D., Uiterwaal C.J.G.J., Fotakis C., Bachau H., Sanchez I., Cormier E. *Phys. Rev. A*, **53**, 2587 (1995).
3. Ganz J., Raab M., Hotop H., Geiger J. *Phys. Rev. Lett.*, **53**, 1547 (1984).
4. Lambropolous P., Zoller P. *Phys. Rev. A*, **379**, 379 (1981).
5. Fedorov M.V., Kazakov A.E. *Progr. Quantum Electron.*, **13**, 1 (1989).
6. Bachau H., Lambropoulos P., Shakeshaft R. *Phys. Rev. A*, **34**, 4785 (1986).
7. Kylstra N.J., van der Hart H.W., Burke P.G., Joachain C.J. *J. Phys. B: At. Mol. Opt. Phys.*, **31**, 3089 (1998).
8. Magunov A.I., Rotter I., Strakhova S.I. *J. Phys. B: At. Mol. Opt. Phys.*, **32**, 1489 (1999).
9. Magunov A.I., Rotter I., Strakhova S.I. *J. Phys. B: At. Mol. Opt. Phys.*, **32**, 1669 (1999).
10. Knight P.L., Lauder M. A., Dalton B. *Phys. Rep.*, **190**, 1 (1990).
11. Böhmer K., Halfmann T., Yatsenko L.P., Charalambidis D., Horsmans A., Bergmann K. *Phys. Rev. A*, **66**, 013406 (2002).
12. Kylstra N.J., Paspalakis E., Knight P.L. *J. Phys. B: At. Mol. Opt. Phys.*, **31**, L719 (1998).
13. Magunov A.I., Rotter I., Strakhova S.I. *J. Phys. B: At. Mol. Opt. Phys.*, **34**, 1489 (2001).
14. Heller Yu.I., Lukinykh V.F., Popov A.K., Slabko V.V. *Phys. Lett.*, **82A**, 4 (1981).
15. Eramo R., Cavalieri S., Fini L., Matera M., DiMauro L.F. *J. Phys. B: At. Mol. Opt. Phys.*, **30**, 3789 (1997).
16. Liao P.F., Bjorklund G.C. *Phys. Rev. A*, **15**, 2009 (1977).
17. Autler S.H., Townes C.H. *Phys. Rev.*, **100**, 703 (1955).
18. Bonch-Bruevich A.M., Khodovoi V.A., Chigir' N.A. *Zh. Eksp. Teor. Fiz.*, **67**, 2069 (1974).